UNIVERSITÀ DI PARMA
ARCHIVIO DELLA RICERCA

University of Parma Research Repository

A mechanistic investigation on kokumi-active γ-Glutamyl tripeptides – A computational study to understand molecular basis of their activity and to identify novel potential kokumi-tasting sequences

note finali coverpage

(Article begins on next page)

24 December 2024

Food Research International

A mechanistic investigation on kokumi-active γ-Glutamyl tripeptides – a computational study to understand molecular basis of their activity and to identify novel potential kokumi-tasting sequences
--Manuscript Draft--

Corresponding Author:	Luca Dellafiora University of Parma ITALY
First Author:	Luca Dellafiora
Order of Authors:	Luca Dellafiora
	Fabio Magnaghi
	Gianni Galaverna
	Chiara Dall'Asta

Abstract:	Kokumi is an important taste perception whose chemical basis still needs clarifications and for which the development of high-throughput tools of analysis is desirable. The activation of Calcium-sensing receptor (CaSR) was described as the molecular initiating event of kokumi perception allowing the use of molecular modelling to deepen its chemical basis and related mechanisms. This study focused on γ-Glutamyl tripeptides, computationally investigated mechanistic basis of their CaSR-activating properties and extended the comprehension of their structure-activity relationship. A library of 400 γ-Glutamyl tripeptides was also screened. γ-Glu-Pro-Ala and γ-Glu-Pro-Ser were identified for further dedicated investigations based on their promising CaSR-activating potential and their presence should be checked accordingly in food matrices to better profile the kokumi fingerprint. This work provided a meaningful tool for the top-down analysis of kokumi-active molecules that may support either the identification of kokumi molecules concealed in food or the rational design of kokumi-active molecules de novo .

Highlights

- Mechanistic and chemical basis of kokumi γ-Glutamyl tripeptides has been depicted
- The stabilization of the closed conformation of Calcium-sensing receptor was modeled
- Specific receptor movements were monitored to assess kokumi activity of molecules
- A virtual library of 400 γ-Glutamyl tripeptides was screened
- γ-Glu-Pro-Ala and γ-Glu-Pro-Ser were described as potential potent kokumi compounds

1   **A mechanistic investigation on kokumi-active γ-Glutamyl tripeptides – a computational**

2   **study to understand molecular basis of their activity and to identify novel potential**

3   **kokumi-tasting sequences**

4

5   Luca Dellafiora[1]*, Fabio Magnaghi[1], Gianni Galaverna[1], Chiara Dall'Asta[1]

6   [1] Department of Food and Drug, University of Parma, Parco Area delle Scienze 27/A, 43124

7   Parma, Italy.

8

9   * Correspondence to: Luca Dellafiora, Department of Food and Drug, University of Parma,

10   Parco Area delle Scienze 27/A, 43124 Parma, Italy. Phone: +39 0521 906070. Email:

11   luca.dellafiora@unipr.it

Abstract

Kokumi is an important taste perception whose chemical basis still needs clarifications and for which the development of high-throughput tools of analysis is desirable. The activation of Calcium-sensing receptor (CaSR) was described as the basis of kokumi perception allowing the use of molecular modelling to deepen its chemical rationale and related mechanisms. This study focused on γ-Glutamyl tripeptides, computationally ~~investigated mechanistic basis~~ providing mechanistic insights on ~~of~~ their CaSR-activating properties and extended the comprehension of their structure-activity relationship. A library of 400 γ-Glutamyl tripeptides was also screened. γ-Glu-Pro-Ala and γ-Glu-Pro-Ser were identified for further dedicated investigations based on their promising CaSR-activating potential and their presence should be checked accordingly in food matrices to better profile the kokumi fingerprint. This work provided a meaningful tool for the top-down analysis of kokumi-active molecules that may support either the identification of kokumi molecules concealed in food or the rational design of kokumi-active molecules *de novo*.

1. Introduction

The term "kokumi" refers to as a complex taste sensation characterized by thickness, mouthfulness and continuity (Toelstede, Dunkel, & Hofmann, 2009; Toelstede & Hofmann, 2008; Zhao, Schieber, & Ganzle, 2016). Such a sensation is important to determine taste, flavour, mouthfeel and aftertaste qualities of a wide variety of foods with critical implications for food acceptance and consequences on consumers behaviour and diet habits (Keast, Costanzo, & Hartley, 2021; Tang, Tan, Teo, & Forde, 2020). For this reason, the identification and characterization of kokumi-active molecules in food is an important piece of information, *inter alia*, to make connections between the chemistry of food and its perception and consumption. At the same time, the design of new kokumi-active molecules meant to be intentionally added in food can be important from a food design standpoint to endow designed food with desired flavour-related properties (e.g. (Ruijschop, Burseg, Lambers, & Overduin, 2009)). However, the kokumi-active fraction is hard to profile with precision in food due to experimental issues, and the *de novo* design of novel kokumi molecules is hampered by the uncomplete understanding of their structure-activity relationship.

From a mechanistic point of view, kokumi perception has been associated with the binding between kokumi-active molecules and the Calcium Sensing Receptor (CaSR), which results in its subsequent allosteric activation (Guha & Majumder, 2022). CaSR is a G-protein coupled receptor (GPCR) consisting in 1078 amino acids and expressed on the surface of diverse cell types. It has been under investigation since its discovery for its involvement in several pathologies (Huang, Zhao, Dong, & Hu, 2021; Sundararaman & van der Vorst, 2021). However, its expression was proved in the gustatory tissues of rats, further demonstrated in the taste buds in lingual epithelia, and the CaSR's involvement was soundly proposed at the

3

basis of kokumi perception (Guha & Majumder, 2022; Maruyama, Yasuda, Kuroda, & Eto, 2012; Ohsu et al., 2010). Specifically, the so called CaSR's Venus fly trap (VFT) domain has been described as the binding site of kokumi substances and its capability to close over ligands has been reported as the molecular initiating event underpinning CaSR activation and kokumi perception (Li, Zhang, & Lametsch, 2022; Wellendorph & Brauner-Osborne, 2009).

Concerning the profiling of taste molecules in food, including kokumi-active compounds, the methods commonly used are still complex and time-consuming. They typically require composite multi-step experimental protocols based on the decomposition of a given matrix followed by the precise description of its taste-active chemical components (J. Kim et al., 2022; Vasilaki, Panagiotopoulou, Koupantsis, Katsanidis, & Mourtzinos). In line with the methods used to identify bioactive peptides of food origin, these methods can be defined "bottom-up" in the sense that they ideally require a comprehensive description of molecules in a certain food followed by their characterization in terms of taste activity (Schrader, 2018). Conversely, "top-down" approaches refer to techniques to create organized (bio)active structures either by etching down a bulk material or by engineering them into specific locations (Smith, Tejeda-Montes, Poch, & Mata, 2011). In the context of bioactive peptides of food origin, "top-down" approaches refer to food matrix-independent methods targeting the identification of bioactive sequences with specific features, the occurrence of which in food is searched after their bioactivity has been proved (Lammi et al., 2021). Similarly, taste-active molecules can be identified using "top-down" approaches defining their potential taste activity first, and then searching their presence in food matrices assessing their role in the overall food taste. In the context of kokumi-active molecules analysis, "top-down" approaches may ensure high-throughput investigations

77   providing ground either to better understand the chemistry underpinning the taste of

78   specific foods *a posteriori*, or to support a knowledge-based design of taste molecules

79   meant to be added in food.

80   In this context, computational analysis proved to efficiently support the characterization of

81   taste molecules (Bo et al., 2022; J. Yang et al., 2021) with promising applications either for a

82   bulk or precise discovery of novel taste-active compounds (Spaggiari, Di Pizio, & Cozzini,

83   2020). In this context, the present work aimed at defining a 3D molecular modelling

84   framework useful for a "top-down" identification of potent kokumi γ-Glutamyl tripeptides

85   to: I) ~~decipher~~ get insights on the chemical and mechanistic basis of potent kokumi-active γ-

86   Glutamyl tripeptides; and ii) to screen a combinatory library of 400 γ-Glutamyl tripeptides to

87   identify novel and potentially potent kokumi-active sequences worthy of further dedicated

88   investigations. The study focused on the class of γ-Glutamyl tripeptides as it includes potent

89   kokumi-active compounds with glutathione (GSH, γ-Glu-Cys-Gly) and γ-Glu-Val-Gly among

90   the most potent kokumi-active molecules described so far (Kuroda et al., 2013; Ohsu et al.,

91   2010). The workflow described here focused on the molecular initiating event of kokumi

92   taste and was based on docking simulations and molecular dynamics to study the

93   interaction between γ-Glutamyl tripeptides and CasR, which has been recently described as

94   the target taste receptor of kokumi molecules (Maruyama et al., 2012). Overall, this work

95   presented a rational, useful and straightforward strategy either to better understand the 3D

96   structure-activity relationship of kokumi-active γ-Glutamyl tripeptides or to identify new,

97   potentially potent, and previously uncharacterized sequences for further analysis.

98

99   **2. Material and methods**

2.1. Construction of γ-Glutamyl tripeptides library, tryptophan and glycine residues

The structures of γ-Glutamyl tripeptides analysed in this study were built using an in-house python script interfaced with PyMol (version 2.3.0; www.pymol.org). All possible duplets of the 20 proteogenic amino acids were generated, for a total of 400 combinations. These elements were symbolically represented by arrays of characters. The generated strings will be then divided into the representative characters of the single amino acid and added sequentially to the gamma carbon of the glutamate. The integrity of the carboxy-terminal was ensured adding an oxygen atom will be added to the carboxy terminal. The entire set of compounds generated was stored in the Protein Data Bank format (.pdb) first and then recursively converted in the Tripos Mol2 format (.mol2) for subsequent analysis using Open Babel (version 3.0.0) (O'Boyle et al., 2011) and setting the protonation state at pH 7 (i.e., carboxy- and ammino-terminal set deprotonated and protonated, respectively). The consistency of binding geometries and bond and atom type assignment were visually inspected before further analysis.

The library included 400 different entries grouping all the possible combinations for γ-Glutamyl tripeptides with a γ-Glutamyl residues at the 1st position (Ammino terminus) and all the possible combinations including permutations of 20 proteinogenic amino acids at the 2nd and 3rd position (Carboxy terminus).

The structure of L-tryptophan (L-Trp) and glycine (Gly) were retrieved from PubChem (S. Kim et al., 2021) in the 3D Structure Data File format (.sdf; CID 6305 and 750, respectively) and further converted in the .mol2 format as described above.

2.2. Ligand-based virtual screening of γ-Glutamyl tripeptides library

123   The library of γ-Glutamyl tripeptides underwent a ligand-based virtual screening to sort

124   entries according to their similarity to γ-Glu-Val-Gly, which is the most potent CaSR-activator

125   γ-Glutamyl tripeptide described *in vitro* so far (Ohsu et al., 2010). The ligand-based virtual

126   screening was done using the LiSiCA (Ligand Similarity using Clique Algorithm) algorithm

127   (Legnik et al., 2015). This algorithm provides a fast ligand-based virtual screening platform

128   to quantify chemical similarities between a reference template (a strong kokumi γ-Glutamyl

129   tripeptide in this case) and a database of target compounds. LiSiCA expresses similarities

130   using the Tanimoto coefficient, a gold standard to quantify chemical analogies. LiSiCA's

131   default parameters were used, with the exception of considering the 3D structures of

132   ligands and setting the maximum allowed atom spatial distance for 3D product graph at 2, in

133   agreement with a previous study (Lammi et al., 2021). This fast virtual screening procedure

134   served to identify a short selection of sequences to carry forth to the slower and more

135   demanding subsequent molecular modelling studies (see below).

136

137   **2.3. CaSR model construction**

138   The 3D model of human CaSR receptor was derived from the crystallographic structure

139   recorded in the Protein Data Bank (https://www.rcsb.org; Berman et al., 2000) with PDB

140   code 5FBK (chain A) (Zhang et al., 2016). This PDB record reported a high-resolution

141   structure of the wild-type extracellular domain of human CaSR (residues 22-539), called

142   venus flytrap (VFT) domain, which binds kokumi active molecules and is involved in the

143   molecular initiating events of kokumi perception (Goralski & Ram, 2022; Mun et al., 2004).

144   Such a structure was chosen based on its high higher resolution (2.10 Å) and more complete

145   set of resolved coordinates compared to the others structure available at the time of

146   analysis (last database access 14th January 2022). However, it presented unresolved

147   coordinates for residues 361-390, which were not available in any of the structures

148   recorded in PDB at the time of analysis (last database access 14th January 2022). This portion

149   consisted in a small peripheral domain the integrity of which was obtained combining data

150   from homology modelling and expert structure editing. In more detail, the whole 3D

151   structure of VTF domain (residues 22-539) was obtained first using trRosetta

152   (https://yanglab.nankai.edu.cn/trRosetta) (J. Y. Yang et al., 2020) using the FASTA sequence

153   of 5FBK structure, in agreement with a previous study (Louisse, Dorne, & Dellafiora, 2022).

154   In more detail, trRosetta is an algorithm for a fast and accurate protein structure prediction

155   that derive protein structures based on direct energy minimizations with a constrained

156   optimization by Rosetta (Simons, Bonneau, Ruczinski, & Baker, 1999). The restraints include

157   inter-residue distance and orientation distributions, predicted by a deep residual neural

158   network. The model provided by trRosetta showed a high confidence with a TM score of 0.9

159   (scores above 0.5 point to correct topological assignment, in agreement with previous

160   studies (J. Y. Yang et al., 2020)). Such model was superimposed to the crystallographic

161   structure and used to tailor the crystallographic structure by substituting the residues 338-

162   402 ensuring the best backbone overlap between the model obtained from homology

163   modelling and the crystallographic structure.

164

165   **2.4. Docking studies**

166   The docking analysis aimed at providing a plausible binding architecture for L-Trp, Gly and

167   the γ-Glutamyl tripeptides under investigation and was performed using the GOLD software

168   (version 2021). The binding site has been defined within a 10-angstrom radius sphere

169   centred at the centroid of the substrate binding site of the VTF domain model with the xyz

170   coordinates set in correspondence with the alpha-carbon of the crystallographic ligands of

171   5FBK (Zhang et al., 2016). Docking protocol was set according to previous studies keeping

172   ligands fully flexible (i.e. all the routable bonds were set free to rotate) and protein semi-

173   flexible allowing polar hydrogens free to rotate (Dellafiora et al., 2017). As a minor

174   modification, 10 poses for each ligand were generated and scored using the internal scoring

175   function GOLDScore as it has been optimized for the prediction of ligand binding positions,

176   according to the manufacturer declaration (https://www.ccdc.cam.ac.uk). Considering that

177   the scoring assignment is proportional to the ligand-pocket fitting (the higher the score, the

178   higher the match to the pocket physico-chemical properties), only the best scored pose for

179   each docked ligand was considered for the analysis, in agreement with previous studies

180   (Dellafiora et al., 2017). Also, the positioning of each ligand was facilitated using the

181   "Similarity constraint" option choosing the crystallographic pose of 5FBK's ligand as

182   template and choosing to avoid the generation of docking poses when the constraint is

183   physically impossible.

184   Moreover, GOLD uses a genetic algorithm that may introduce variability in the score

185   assignment. Therefore, each ligand was run in triplicate to check the respective scoring

186   fluctuations. Score assignment was found reliably stable for active compounds (further

187   details are reported in the Results and Discussion section) with a maximum coefficient of

188   variation below 0.9 % (scores are expressed as mean ± standard deviation).

189   RMSD values between the calculated and crystallographic poses of L-Trp were calculated

190   using the align command implemented in PyMol disallowing cycles correction and

191   considering the all set of not-hydrogen atoms.

192

193   **2.5. Pharmacophoric analysis**

194   The pocket of VFT domain was defined using GetCleft (Gaudreault, Morency, &

195   Najmanovich, 2015), while the respective pharmacophoric fingerprint was derived using the

196   IsoMIF algorithm (Chartier & Najmanovich, 2015), as previously described (Lammi et al.,

197   2021).

198

199   **2.6. Molecular dynamics**

200   Molecular dynamics aimed at studying the stability of VTF domain in complex with the

201   various ligands over the time. They were performed using GROMACS (version 2019.4)

202   (Abraham et al., 2015) with CHARMM27 all-atom force field parameters support (Best et al.,

203   2012) for protein, L-Trp and Gly. γ-Glutamyl tripeptides have been processed and

204   parameterized with CHARMM27 all-atom force field using the SwissParam tool

205   (http://www.swissparam.ch) (Zoete, Cuendet, Grosdidier, & Michielin, 2011). Input

206   structures were solvated with SPCE waters in a cubic periodic boundary condition, and

207   counter ions (Na^+ or Cl^-) were added to neutralize the system. Prior to running simulations,

208   each system was energetically minimized to avoid steric clashes and to correct improper

209   geometries using the steepest descent algorithm with a maximum of 5,000 steps.

210   Afterwards, all the systems underwent isothermal (300 K, coupling time 2 psec) and isobaric

211   (1 bar, coupling time 2 psec) 100 psec simulations before running 25 nsec simulations (300 K

212   with a coupling time of 0.1 psec and 1 bar with a coupling time of 2.0 psec).

213

214   **3. Results and Discussion**

215   Kokumi perception is a complex phenomenon, and its underpinning early mechanisms

216   depend on the activation of CaSR. CaSR is a class C G protein-coupled receptor (GPCR)

217   working as a homodimer with a large extracellular VFT domain, which is involved in the

218   recognition of kokumi active molecules (Ling et al., 2021). The network of molecular

219   mechanisms underpinning the activation of CaSR and the transduction of signal through the

220   membrane is complex and still need clarifications. However, the capability of VFT domain to

221   close over ligands has been described as the molecular initiating event underpinning CaSR

222   activation and kokumi perception (Wellendorph & Brauner-Osborne, 2009). On this basis,

223   the present work assessed whether a computational workflow could estimate the capability

224   of ligands to elicit a kokumi perception by triggering the very early mechanism at the basis

225   of kokumi taste, i.e. the stabilization of the closed and active structure of CaSR VFT domain.

226   In this respect, computational methods and bioinformatics already succeeded to investigate

227   taste peptides (Iwaniak, Minkiewicz, Darewicz, & Hrynkiewicz, 2016). Specifically, in this

228   work, a 3D molecular modelling approach was used combining docking studies,

229   pharmacophoric analysis and molecular dynamics simulations to: i) ~~understand~~ get insights

230   on the chemical basis of VFT domain-kokumi molecule interaction; and ii) study the early

231   molecular mechanisms of receptor activation over the time. Once assessed the model

232   performances, a virtual library of 400 γ-Glutamyl tripeptides was screened to identify novel

233   and potentially strong kokumi-active sequences never described before.

3.1. Assessment of model performances

235   Model performances were assessed following a multi-tier approach in agreement with

236   previous studies (e.g., (Louisse et al., 2022)). First, the capability to reproduce the binding

237   architecture of L-Trp, taken as a kokumi reference ligand (Laffitte et al., 2021), was done

238   comparing its calculated pose with the crystallographic architecture of binding reported in

239   the PDB structure having code 7DTU (Ling et al., 2021). As shown in Figure 1, docking

240   simulation was able to reliably reproduce the binding architecture of L-Trp and its network

241   of polar interactions, with an average RMSD value of 0.6 Å, confirming the geometrical

242   reliability of the model. Then, the capability of model to discriminate between CaSR ligands

243   (i.e., kokumi molecules) and non-ligands (i.e., kokumi-inactive molecules) was assessed

244   combining data from docking studies and molecular dynamic simulations. Specifically, the

245   weak CaSR activator Gly (chosen as negative controls due to its negligible kokumi activity),

246   the moderate CaSR activator and kokumi-active molecules L-Trp, the strong activator and

247   kokumi-active molecule γ-Glu-Val-Gly and the inactive γ-Glu-Val-Trp (chosen as a negative

248   control) were considered in this study (Conigrave, Quinn, & Brown, 2000; Geng et al., 2016;

249   Ohsu et al., 2010; Zhao et al., 2016). As shown in Table 1, the whole set of molecules

250   included in this study recorded relatively high docking scores pointing to their possible

251   capability to match pocket requirements (the higher the score, the higher the theoretical

252   capability of ligands to match the pocket). Conversely, the inspection of docking poses

253   revealed a substantial difference between the weak-to-strong activators (Gly, L-Trp and γ-

254   Glu-Val-Gly) and the inactive sequence γ-Glu-Val-Trp. Specifically, the formers showed an

255   architecture of binding that resembled the crystallographic pose of L-Trp with the alpha

256   carboxy- and amino-group of γ-Glutamyl residue involved in polar contact with Ser147,

257   Ala168 and Ser170 (Figure 2). The comparison between the docking poses and the

258   pharmacophoric analysis of the binding pocket provided a mechanistic rationale for the

259   experimental data reported so far for this set of molecules. In particular, the higher

260   capability of L-Trp to activate CaSR compared to Gly could be explained, at least in part, by

261   the better capability of the former to interact with the VFT domain. Indeed, the indole ring

262 of L-Trp was arranged within a hydrophobic region of the binding site likely adding

263 additional hydrophobic/hydrophobic favourable interactions compared to Gly. In this

264 respect, Gly recorded a docking score significantly lower than the other molecules, in

265 agreement with its very weak capability to activate CaSR. These additional contributions to

266 the binding event of L-Trp could suggest a major effect to stabilize the closed conformation

267 of VTF domain compared to Gly determining a more effective CaSR activation and a more

268 pronounced kokumi perception, in agreement with previous studies (Mun et al., 2004;

269 Goralsky and Ram, 2022). Following this line of interpretation, the stronger activity of γ-Glu-

270 Val-Gly could be explained by the additional contribution to the binding event due to the

271 polar contact between its Gly C-terminus and the side chain of Asn102 (Figure 2C).

272 Conversely, γ-Glu-Val-Trp, which was described as unable to activate CaSR (Ohsu et al.,

273 2010), showed a substantially different architecture of binding which missed all the key

274 contacts described above and reported in crystallographic studies despite the high score

275 recorded. The incapability to mimic the binding pose of γ-Glu-Val-Gly was due to the local

276 lack of a sufficient space to receive the bulky side chain of Trp at the 3rd (C-terminal)

277 position that forced this peptide to find an alternative arrangement into the pocket. The

278 relatively high score was reasonably due to the high number of hydrophobic/hydrophobic

279 contributions. However, an appreciable interaction with VFT domain was not deemed likely

280 based on the lack of the network of key polar contacts well reported by crystallographic

281 records and calculated for γ-Glu-Val-Gly. In addition, γ-Glu-Val-Trp recorded more variable

282 scores compared to the other ligands considered here, with a coefficient of variation (CV) of

283 3.6 % while the other activators showed CV values below 1%. The higher variability of γ-Glu-

284 Val-Trp scores could indicate the incapability to find a unique and stable binding

285 architecture, which is typically associated with nonoptimal ligands that are unable to

286   satisfyingly match pocket requirements (Aichinger et al., 2020). Taken together these results

287   pointed to the possible relevance and usability of docking scores and poses to distinguish

288   CaSR activators from inactive molecules.

289   Keeping in mind that the stabilization of the closed conformation of VFT domain is a key

290   mechanistic event underpinning CaSR activation and kokumi taste perception, the stability

291   of VFT domain in complex with Gly, L-Trp, γ-Glu-Val-Gly and γ-Glu-Val-Trp or in the unbound

292   state was monitored over the time with molecular dynamic simulations. In particular, the

293   protein's α-carbon root mean squared deviation (RMSD) was measured along with specific

294   inter-molecular movements to describe VFT opening/closure (Figure 3). Specifically, three

295   inter-atomic distances were considered to monitor VFT domain's motions and to describe

296   either the stable maintenance of a closed conformation or its opening preluding to ligand

297   detachment and receptor inactivation (Figure 3). With respect to the RMSD analysis, the

298   complexes considered and the VFT domain in the unbound state showed a similar trend

299   similar, although the complex with γ-Glu-Val-Trp showed slightly higher values from 15

300   nanoseconds onward (Figure 1S; Supporting material). This might point to a slight less stable

301   geometrical organization of the complex with γ-Glu-Val-Trp compared to the other ligands

302   or to the unbound VFT domain. Concerning the intra-molecular distances considered to

303   monitor VFT domain closure/opening, a clearly different trend was observed for moderate

304   and strong activators (i.e., L-Trp and γ-Glu-Val-Gly) compared to the weak activator Gly, the

305   inactive peptide γ-Glu-Val-Trp and the unbound VFT domain. As shown in Figure 3B, the

306   strong activator γ-Glu-Val-Gly and the moderate activator L-Trp showed a similar trend in

307   the three intra-molecular contact regions (C1, C2 and C3) considered, which were kept

308   tightly close along the whole simulation. Conversely, an early detachment was observed for

309   all the contact regions in the unbound VFT domain (more marked for C2 than C1 or C3)

310 pointing as unfavourable the closed geometry of VFT domain in the unbound state, in

311 agreement with previous studies (Ling et al., 2021). Of note, monitoring such intra-

312 molecular distances could provide a semi-quantitative comparison of ligands in terms of

313 activity: the very weak activator Gly showed for the three contact point regions considered

314 a trend that was intermediate between the inactive sequence γ-Glu-Val-Trp and the two

315 activators L-Trp and γ-Glu-Val-Gly. This was particularly evident for C2 and C3 where the

316 interatomic distances tended to resemble the scenario drawn for the unbound VFT domain.

317 In other words, Gly showed a limited capability to stabilize the closed conformation of VFT

318 domain causing its opening as time went by during the simulation. This outcome could

319 provide a mechanistic basis to better understand the rationale for the very weak activity

320 reported for Gly. Concerning the inactive peptide γ-Glu-Val-Trp, all the interatomic distances

321 considered constantly increased during the simulation pointing to a clear opening of the VFT

322 domain. The close inspection of complex trajectories confirmed such hypothesis as constant

323 opening movements were observed for all the contact regions considered (Figure 3C). As

324 described above for Gly, this evidence provided a mechanistic rationale to understand the

325 molecular basis underpinning the incapability of γ-Glu-Val-Trp to activate CaSR.

326 Taken together, these results highlighted the usability of the 3D modelling presented to

327 investigate the early molecular event of kokumi perception and described a combination of

328 docking simulations, pharmacophoric analysis and molecular dynamics as a meaningful tool

329 to estimate the CaSR-activating potential of γ-Glutamyl tripeptides. At the same time,

330 although the moderate activator L-Trp was not distinguished from the stronger γ-Glu-Val-

331 Gly peptide preventing the possibility to directly correlate computational results to

332 experimental values (e.g. EC_{50}), the reliability to semi-quantitatively estimate the CaSR-

333 activating potential of γ-Glutamyl peptides was pointed out. Specifically, the procedure

15

334   proved efficacy to soundly distinguish moderate-to-strong γ-Glutamyl peptides from weak

335   or inactive molecules.

336   **3.2. Virtual screening of γ-Glutamyl peptides library**

337   Based on the reliability of modelling framework discussed above, a virtual library grouping

338   400 γ-Glutamyl tripeptides was screened to identify novel sequences with a high theoretical

339   potential as CaSR activators to study in further dedicated investigations. To this end, a

340   ligand-based virtual screening was done to pre-filter the library and identify few promising

341   candidates to investigate with docking simulations and molecular dynamics. Such pre-

342   screening was done using a ligand-based fast search with LiSiCA algorithm and using γ-Glu-

343   Val-Gly as reference template. LiSiCA scores ideally range from 0 (no similarity found) to 1

344   (high similarity found) and sorted γ-Glutamyl tripeptides according to their chemical

345   similarity to γ-Glu-Val-Gly, which is one of the most potent CaSR activator and kokumi-active

346   molecule described so far. The rationale of this choice was that chemical similarities may

347   ensure a certain degree of conservation in terms of biological activity (CaSR-activating and

348   kokumi properties in this case), as previously demonstrated (Lammi et al., 2021). The virtual

349   screening results for the entire library of 400 γ-Glu-peptides are reported in Table 1S,

350   Supporting material. Of note, 90% of the most potent γ-Glutamyl peptides described by

351   Osho and co-workers (Osho et al., 2010) (i.e., with a reported CaSR activity < 30 μM) were at

352   the top of LiSiCA rank with scores above 0.8 (Table 1S; Supporting material). This evidence

353   validated the use of γ-Glu-Val-Gly as a template to search potent CaSR-activating γ-Glutamyl

354   tripeptides and to enrich the top region of LiSiCA hierarchization with highly potent

355   sequences.

356   Then, a selection of top-ranked sequences was considered for further analysis with docking

357   studies and molecular dynamics. Among the uncharacterized sequences in terms of CaSR

358   activity at the time of analysis and to the best of our knowledge, γ-Glu-Pro-Ala, γ-Glu-Ile-Ala,

359   γ-Glu-Pro-Ser, γ-Glu-Ile-Cys and γ-Glu-Ile-Pro were chosen based on their sequence

360   analogies to highly potent sequences already described (Table 1S; Supporting material) to

361   maximize the chance to identify novel potent CaSR-activating γ-Glutamyl tripeptides. As

362   shown in Figure 2, and despite the relatively high and stable scores recorded (Table 1), γ-

363   Glu-Ile-Cys and γ-Glu-Ile-Pro showed a pose similar to the inactive peptide γ-Glu-Val-Trp.

364   Therefore, their pose was considered not promising to stabilize a closed conformation of

365   VFT domain and were not considered for further analysis. Conversely, γ-Glu-Pro-Ala, γ-Glu-

366   Ile-Ala and γ-Glu-Pro-Se showed a binding pose similar to γ-Glu-Val-Gly and drawn a

367   comparable network of polar interactions with the pocket suggesting that they could

368   efficiently stabilize the closed conformation of VFT domain. This hypothesis was further

369   assessed with molecular dynamic simulations. As shown in Figure 3D, γ-Glu-Ile-Ala caused

370   an opening of the VFT domain as suggested by the increase of interatomic distances at the

371   contact regions C1, C2 and C3. On this basis, it was not deemed to be a potent CaSR-

372   activating peptide. Conversely, the interaction of γ-Glu-Pro-Ala and γ-Glu-Pro-Ser

373   determined the stable closure of the receptor over the time, and they were both considered

374   theoretically potent CaSR-activating and kokumi-tasting γ-Glutamyl peptides worthy of

375   further dedicated analysis. Of note, γ-Glu-Pro-Ala showed a closure tighter than both γ-Glu-

376   Pro-Ser and γ-Glu-Val-Gly at the contact region C3 possibly pointing to a marked capability

377   to stabilize the closed conformation of VTF domain with possible consequences on its

378   kokumi perception.

379   From a general point of view, the lack of appreciable activity calculated for γ-Glu-Ile-Ala, γ-

380   Glu-Ile-Cys and γ-Glu-Ile-Pro agreed with the data available so far in terms of potent CaSR-

381   activating γ-Glutamyl tripeptides. Indeed, among the most potent sequences reported so

382   far, the 2nd position of γ-Glutamyl tripeptides is rarely occupied by bulky residues and Ile is

383   reported at the 2nd position in the reference set of already characterized γ-Glutamyl

384   tripeptides (Table 1S; Supporting material) only in one moderately active sequence (γ-Glu-

385   Ile-Gly). This evidence is in line with the observed limited space the pocket had to receive

386   the side chain of residues at the 2nd position (Figure 4A). This structural requirement was

387   reasonably at the basis of the VFT domain opening to allow the arrangement of the bulky

388   side chain at the 2nd position of γ-Glu-Ile-Ala and might generally determine either a low or

389   no activation of CaSR by γ-Glutamyl tripeptide with bulky side chains at the 2nd position.

390   Conversely, less bulky side chains, like Val, or Pro or Cys, could be better tolerated at the 2nd

391   position, and they may efficiently stabilize the closed and active conformation of VFT

392   domain, in line with the evidence reported for the reference set of γ-Glutamyl tripeptides

393   (Table 1S; Supporting material). Specifically, although the pharmacophoric analysis revealed

394   regions able to receive polar groups (Figure 3S; Supporting material), steric constraints at

395   the 2nd position seemed important to determine the capability of γ-Glutamyl tripeptide to

396   properly bind the VFT, in line with the lack of potent kokumi γ-Glutamyl tripeptide with a

397   bulky polar residue at the 2nd position (Table 1S; Supporting material). In this respect, the

398   reference set of γ-Glutamyl tripeptides (Table 1S; Supporting material) included only one

399   kokumi active peptide with a polar (and small) residue at the 2nd position, i.e. γ-Glutamyl-

400   Thr-Gly, further supporting this hypothesis. Concerning the space receiving the side chains

401   in 3rd position (C-terminus), the analysis of VFT domain binding site revealed an opening to a

402   solvent exposed region (Figure 4B) that could explain the higher tolerance for bulky side

403   chains as observed for some CaSR-activating γ-Glutamyl tripeptides (e.g., γ-Glu-Val-Phe and

404   γ-Glu-Val-Arg, Table 1S; Supporting material). Nonetheless, the existence of a certain

405   specificity could be inferred considering the incapability of γ-Glu-Val-Trp to properly dock

406   the binding site and to active CaSR.

407

408   **4. Conclusion**

409   The identification of kokumi molecules, although still challenging, is important to

410   understand the chemistry of food and related consequences on diet habits and consumer

411   behaviour. The recent advances in the comprehension of mechanisms underpinning kokumi

412   perception, and in particular the identification of CaSR as the receptor responsible for

413   kokumi molecules recognition, paved the way to use molecular modelling approaches as a

414   meaningful tool of analysis. In this context, the present work showed that modelling the

415   interaction with the CaSR's VFT domain could efficiently estimate the activating potential of

416   γ-Glutamyl tripeptides. In particular, the study identified relevant early mechanistic features

417   at the basis of CaSR activation, such as the way γ-Glutamyl tripeptides arranged into the

418   binding site and the related effects on VFT domain opening, that could be efficiently

419   modelled to extend knowledge on understand the chemistry of γ-Glutamyl tripeptides and

420   used to estimate the potential of still uncharacterized sequences. This may be used in future

421   bulk analysis for a systematic and high throughput analysis supporting the characterization

422   of taste molecules in food. In addition, this study described precisely structural features

423   affecting CaSR-activating potential of γ-Glutamyl tripeptides and the 3D structure-activity

424   relationship analysis could serve as a useful blueprint to improve the understanding of

425   chemical basis for kokumi molecules. Also assessing the interaction between the γ-Glutamyl

19

426 tripeptide under analysis and other GPCRs might be considered for further analysis to better

427 characterize the biological activity beyond their taste properties, in line with the various

428 activity they may exert in living organisms (Lu et al., 2021).

429 Overall, this work provided a useful, reliable and high-throughput tool for a top-down

430 screening of γ-Glutamyl tripeptides which may be integrated into the conventional

431 characterization and sensory tests of taste molecules facilitating the fingerprinting of

432 kokumi compounds in food. Similarly, the model could help the rational design of libraries of

433 compounds in the context of the *de novo* synthesis of kokumi molecules.

434 Finally, two molecules with a high potential in terms of CaSR activating properties and

435 kokumi taste were identified (i.e., γ-Glu-Pro-Ala and γ-Glu-Pro-Ser). Although such

436 molecules have been prioritized for further dedicated investigations and sensory tests to

437 ultimately verify their actual kokumi properties, it is advised their inclusion in the list of

438 molecules to check in food matrices to characterize their possible kokumi fingerprint at a

439 molecular level.

440

441 **Declaration of interest**

442 The authors have nothing to disclose.

443

444 **Acknowledgment**

447

448 **References**

449 Abraham, M. J., Murtola, T., Schulz, R., Páll, S., Smith, J. C., Hess, B., & Lindahl, E. (2015). GROMACS:

450   High performance molecular simulations through multi-level parallelism from laptops to

451   supercomputers. *SoftwareX, 1-2*, 19-25.

452 Aichinger, G., Dellafiora, L., Pantazi, F., Del Favero, G., Galaverna, G., Dall'Asta, C., & Marko, D.

453   (2020). Alternaria toxins as casein kinase 2 inhibitors and possible consequences for

454   estrogenicity: a hybrid in silico/in vitro study. *Archives of Toxicology, 94* (6), 2225-2237.

455 Best, R. B., Zhu, X., Shim, J., Lopes, P. E. M., Mittal, J., Feig, M., & MacKerell, A. D. (2012).

456   Optimization of the Additive CHARMM All-Atom Protein Force Field Targeting Improved

457   Sampling of the Backbone phi, psi and Side-Chain chi(1) and chi(2) Dihedral Angles. *Journal*

458   *of Chemical Theory and Computation, 8* (9), 3257-3273.

459 Bo, W., Qin, D., Zheng, X., Wang, Y., Ding, B., Li, Y., & Liang, G. (2022). Prediction of bitterant and

460   sweetener using structure-taste relationship models based on an artificial neural network.

461   *Food Research International, 153*, 110974.

462 Chartier, M., & Najmanovich, R. (2015). Detection of Binding Site Molecular Interaction Field

463   Similarities. *Journal of Chemical Information and Modeling, 55* (8), 1600-1615.

464 Conigrave, A. D., Quinn, S. J., & Brown, E. M. (2000). L-Amino acid sensing by the extracellular Ca2+-

465   sensing receptor. *Proceedings of the National Academy of Sciences of the United States of*

466   *America, 97* (9), 4814-4819.

467 Dellafiora, L., Ruotolo, R., Perotti, A., Cirlini, M., Galaverna, G., Cozzini, P., Buschini, A., & Dall'Asta, C.

468   (2017). Molecular insights on xenoestrogenic potential of zearalenone-14-glucoside through

469   a mixed in vitro/in silico approach. *Food and Chemical Toxicology, 108*, 257-266.

470 Gaudreault, F., Morency, L. P., & Najmanovich, R. J. (2015). NRGsuite: a PyMOL plugin to perform

471   docking simulations in real time using FlexAID. *Bioinformatics, 31* (23), 3856-3858.

472 Geng, Y., Mosyak, L., Kurinov, I., Zuo, H., Sturchler, E., Cheng, T. C., Subramanyam, P., Brown, A. P.,

473   Brennan, S. C., Mun, H. C., Bush, M., Chen, Y., Nguyen, T. X., Cao, B. H., Chang, D. D., Quick,

474   M., Conigrave, A. D., Colecraft, H. M., McDonald, P., & Fan, Q. R. (2016). Structural

475   mechanism of ligand activation in human calcium-sensing receptor. *Elife, 5*.

476 Goralski, T., & Ram, J. L. (2022). Extracellular Calcium Receptor as a Target for Glutathione and Its

477   Derivatives. *International Journal of Molecular Sciences, 23* (2).

478 Guha, S., & Majumder, K. (2022). Comprehensive Review of γ-Glutamyl Peptides (γ-GPs) and Their

479   Effect on Inflammation Concerning Cardiovascular Health. *Journal of Agricultural and Food*

480   *Chemistry*.

481 Huang, L., Zhao, Y. J., Dong, Q. R., & Hu, G. C. (2021). A study of altered calcium sensing system

482   caused primary membranous nephropathy to end-stage renal failure. *Biomedicine &*

483   *Pharmacotherapy, 141*.

484 Iwaniak, A., Minkiewicz, P., Darewicz, M., & Hrynkiewicz, M. (2016). Food protein-originating

485   peptides as tastants - Physiological, technological, sensory, and bioinformatic approaches.

486   *Food Research International, 89*, 27-38.

487 Keast, R., Costanzo, A., & Hartley, I. (2021). Macronutrient Sensing in the Oral Cavity and

488   Gastrointestinal Tract: Alimentary Tastes. *Nutrients, 13* (2).

489 Kim, J., Ahmad, R., Deb-Choudhury, S., Subbaraj, A., Dalziel, J. E., & Knowles, S. O. (2022). Generation

490   and identification of kokumi compounds and their validation by taste-receptor assay: An

491   example with dry-cured lamb meat. *Food Chemistry: X, 13*, 100218.

492 Kim, S., Chen, J., Cheng, T. J., Gindulyte, A., He, J., He, S. Q., Li, Q. L., Shoemaker, B. A., Thiessen, P.

493   A., Yu, B., Zaslavsky, L., Zhang, J., & Bolton, E. E. (2021). PubChem in 2021: new data content

494   and improved web interfaces. *Nucleic Acids Research, 49* (D1), D1388-D1395.

495 Kuroda, M., Kato, Y., Yamazaki, J., Kai, Y., Mizukoshi, T., Miyano, H., & Eto, Y. (2013). Determination

496   and quantification of the kokumi peptide, gamma-glutamyl-valyl-glycine, in commercial soy

497   sauces. *Food Chemistry, 141* (2), 823-828.

498 Laffitte, A., Gibbs, M., de Alvaro, C. H., Addison, J., Lonsdale, Z. N., Giribaldi, M. G., Rossignoli, A.,

499   Vennegeerts, T., Winnig, M., Klebansky, B., Skiles, J., Logan, D. W., & McGrane, S. J. (2021).

Kokumi taste perception is functional in a model carnivore, the domestic cat (Felis catus). *Scientific Reports, 11* (1).

Lammi, C., Boschin, G., Bollati, C., Arnoldi, A., Galaverna, G., & Dellafiora, L. (2021). A heuristic, computer-driven and top-down approach to identify novel bioactive peptides: A proof-of-principle on angiotensin I converting enzyme inhibitory peptides. *Food Research International, 150.*

Legnik, S., Stular, T., Brus, B., Knez, D., Gobec, S., Janezic, D., & Konc, J. (2015). LiSiCA: A Software for Ligand-Based Virtual Screening and Its Application for the Discovery of Butyrylcholinesterase Inhibitors. *Journal of Chemical Information and Modeling, 55* (8), 1521-1528.

Li, Q., Zhang, L. T., & Lametsch, R. (2022). Current progress in kokumi-active peptides, evaluation and preparation methods: a review. *Critical Reviews in Food Science and Nutrition, 62* (5), 1230-1241.

Ling, S. L., Shi, P., Liu, S. L., Meng, X. Y., Zhou, Y. X., Sun, W. J., Chang, S. H., Zhang, X., Zhang, L. H., Shi, C. W., Sun, D. M., Liu, L., & Tian, C. L. (2021). Structural mechanism of cooperative activation of the human calcium-sensing receptor by Ca2+ ions and L-tryptophan. *Cell Research, 31* (4), 383-394.

Louisse, J., Dorne, J. L. C. M., & Dellafiora, L. (2022). Investigating the interaction between organic anion transporter 1 and ochratoxin A: An in silico structural study to depict early molecular events of substrate recruitment and the impact of single point mutations. *Toxycology Letters, 355*, 19-30.

Lu, Y. J., Wang, J., Soladoye, O. P., Aluko, R. E., Fu, Y., & Zhang, Y. H. (2021). Preparation, receptors, bioactivity and bioavailability of gamma-glutamyl peptides: A comprehensive review. *Trends in Food Science & Technology, 113*, 301-314.

Maruyama, Y., Yasuda, R., Kuroda, M., & Eto, Y. (2012). Kokumi Substances, Enhancers of Basic Tastes, Induce Responses in Calcium-Sensing Receptor Expressing Taste Cells. *Plos One, 7* (4).

23

525   Mun, H. C., Franks, A. H., Culverston, E. L., Krapcho, K., Nemeth, E. F., & Conigrave, A. D. (2004). The

526   Venus fly trap domain of the extracellular Ca2+-sensing receptor is required for L-amino acid

527   sensing. *Journal of Biological Chemistry, 279* (50), 51739-51744.

528   O'Boyle, N. M., Banck, M., James, C. A., Morley, C., Vandermeersch, T., & Hutchison, G. R. (2011).

529   Open Babel: An open chemical toolbox. *Journal of Cheminformatics, 3.*

530   Ohsu, T., Amino, Y., Nagasaki, H., Yamanaka, T., Takeshita, S., Hatanaka, T., Maruyama, Y.,

531   Miyamura, N., & Eto, Y. (2010). Involvement of the Calcium-sensing Receptor in Human

532   Taste Perception. *Journal of Biological Chemistry, 285* (2), 1016-1022.

533   Ruijschop, R., Burseg, K. M. M., Lambers, T. T., & Overduin, J. (2009). Designing foods to induce

534   satiation: a flavour perspective. In D. J. McClements & E. A. Decker (Eds.), *Designing*

535   *Functional Foods: Measuring and Controlling Food Structure Breakdown and Nutrient*

536   *Absorption* (pp. 623-646).

537   Schrader, M. (2018). Origins, Technological Development, and Applications of Peptidomics. In M.

538   Schrader & L. Fricker (Eds.), *Peptidomics: Methods and Strategies* (Vol. 1719, pp. 3-39).

539   Simons, K. T., Bonneau, R., Ruczinski, I., & Baker, D. (1999). Ab initio protein structure prediction of

540   CASP III targets using ROSETTA. *Proteins-Structure Function and Bioinformatics*, 171-176.

541   Smith, K. H., Tejeda-Montes, E., Poch, M., & Mata, A. (2011). Integrating top-down and self-assembly

542   in the fabrication of peptide and protein-based biomedical materials. *Chemical Society*

543   *Reviews, 40* (9), 4563-4577.

544   Spaggiari, G., Di Pizio, A., & Cozzini, P. (2020). Sweet, umami and bitter taste receptors: State of the

545   art of in silico molecular modeling approaches. *Trends in Food Science & Technology, 96*, 21-

546   29.

547   Sundararaman, S. S., & van der Vorst, E. P. C. (2021). Calcium-Sensing Receptor (CaSR), Its Impact on

548   Inflammation and the Consequences on Cardiovascular Health. *International Journal of*

549   *Molecular Sciences, 22* (5).

550   Tang, C. S., Tan, V. W. K., Teo, P. S., & Forde, C. G. (2020). Savoury and kokumi enhancement

551   increases perceived calories and expectations of fullness in equicaloric beef broths. *Food*

552   *Quality and Preference, 83*.

553   Toelstede, S., Dunkel, A., & Hofmann, T. (2009). A Series of Kokumi Peptides Impart the Long-Lasting

554   Mouthfulness of Matured Gouda Cheese. *Journal of Agricultural and Food Chemistry, 57* (4),

555   1440-1448.

556   Toelstede, S., & Hofmann, T. (2008). Sensomics mapping and identification of the key bitter

557   metabolites in Gouda cheese. *Journal of Agricultural and Food Chemistry, 56* (8), 2795-2804.

558   Vasilaki, A., Panagiotopoulou, E., Koupantsis, T., Katsanidis, E., & Mourtzinos, I. Recent insights in

559   flavor-enhancers: Definition, mechanism of action, taste-enhancing ingredients, analytical

560   techniques and the potential of utilization. *Critical Reviews in Food Science and Nutrition*.

561   Wellendorph, P., & Brauner-Osborne, H. (2009). Molecular basis for amino acid sensing by family C

562   G-protein-coupled receptors. *British Journal of Pharmacology, 156* (6), 869-884.

563   Yang, J., Huang, Y. R., Cui, C., Dong, H., Zeng, X. F., & Bai, W. D. (2021). Umami-enhancing effect of

564   typical kokumi-active gamma-glutamyl peptides evaluated via sensory analysis and

565   molecular modeling approaches. *Food Chemistry, 338*.

566   Yang, J. Y., Anishchenko, I., Park, H., Peng, Z. L., Ovchinnikov, S., & Baker, D. (2020). Improved

567   protein structure prediction using predicted interresidue orientations. *Proceedings of the*

568   *National Academy of Sciences of the United States of America, 117* (3), 1496-1503.

569   Zhang, C., Zhang, T., Zou, J., Miller, C. L., Gorkhali, R., Yang, J. Y., Schilmiller, A., Wang, S., Huang, K.,

570   Brown, E. M., Moremen, K. W., Hu, J., & Yang, J. J. (2016). Structural basis for regulation of

571   human calcium-sensing receptor by magnesium ions and an unexpected tryptophan

572   derivative co-agonist. *Science Advances, 2* (5).

573   Zhao, C. J., Schieber, A., & Ganzle, M. G. (2016). Formation of taste-active amino acids, amino acid

574   derivatives and peptides in food fermentations - A review. *Food Research International, 89*,

575   39-47.

576   Zoete, V., Cuendet, M. A., Grosdidier, A., & Michielin, O. (2011). SwissParam: A Fast Force Field

577   Generation Tool for Small Organic Molecules. *Journal of Computational Chemistry, 32* (11),

578   2359-2368.

579

581
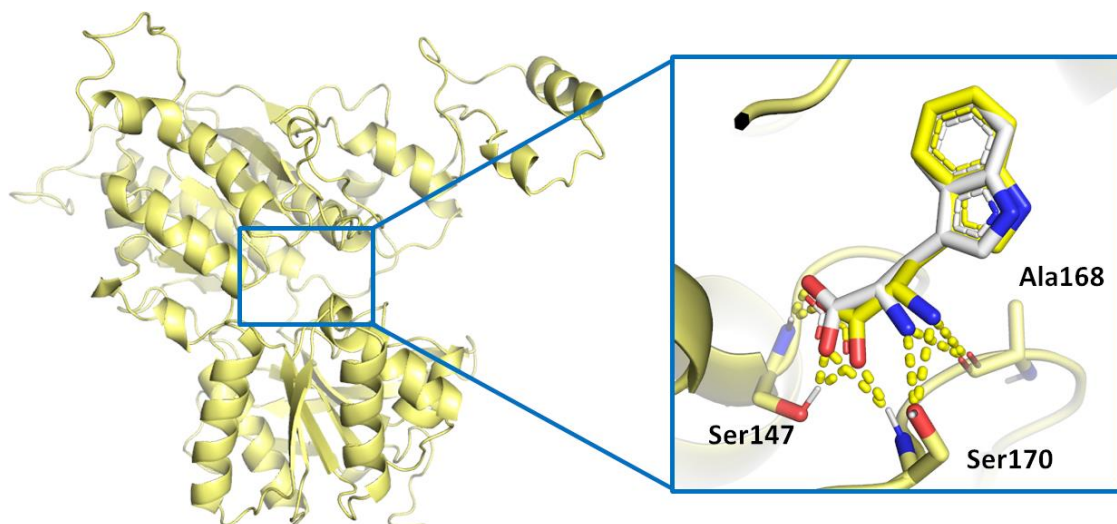
Figure 1. Graphical representation of CaSR VTF domain. The protein is represented in cartoon while ligands are represented in stick. The close-up on the right reports the comparison between the calculated (yellow) and crystallographic (white) pose of L-Trp. Yellow dashed lined indicate to formation of polar contacts.
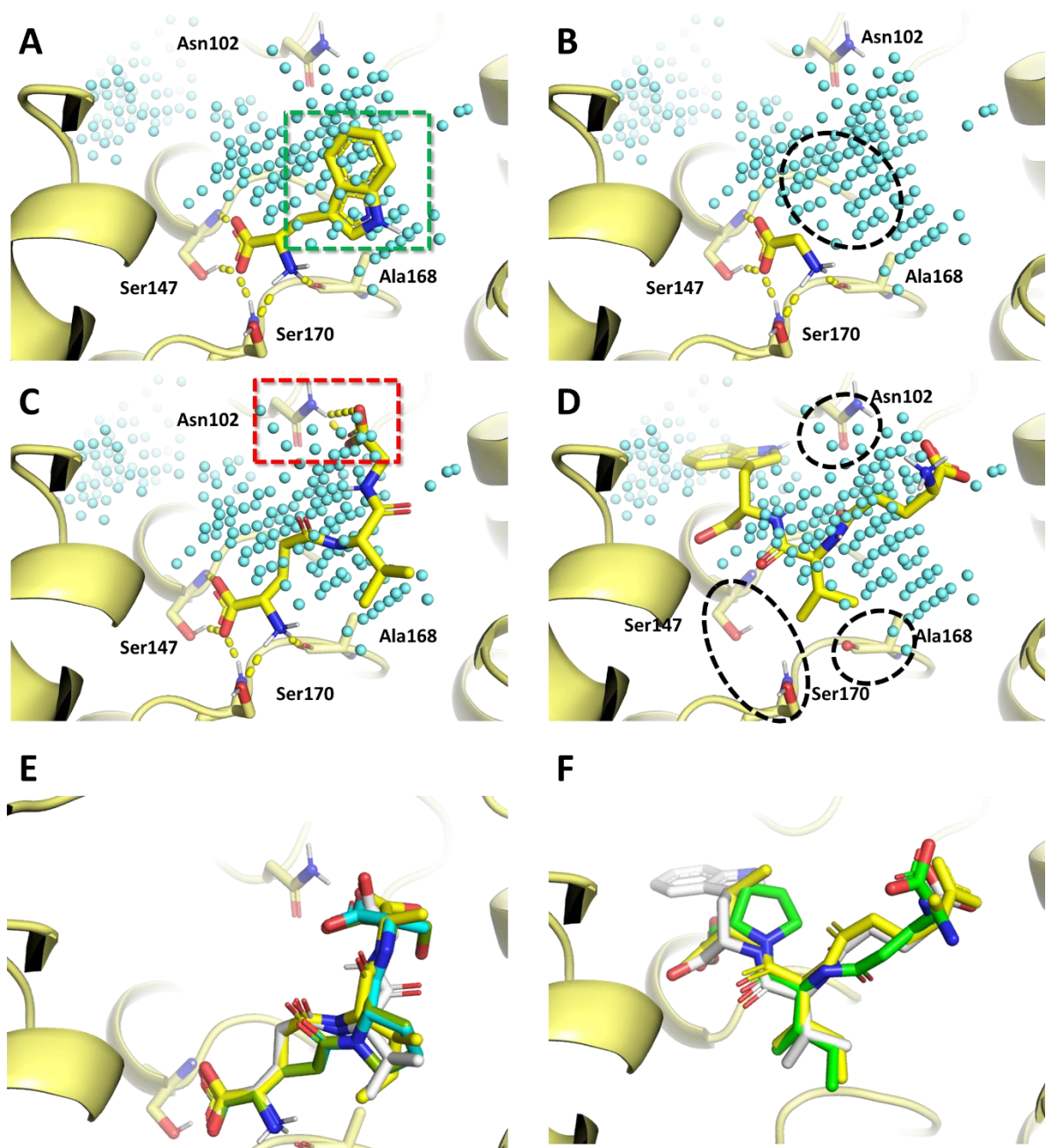
Figure 2. Docking pose of molecules under investigation. The protein is represented in

cartoon while ligands and protein's amino acids involved in polar contacts are represented

in sticks. Yellow dashed lines indicate polar contacts while cyan spheres represent the

region of the binding pocket energetically suitable to receive hydrophobic groups. **A.** L-Trp.

The green dashed box indicates the proper arrangement of the hydrophobic indole ring

within a region of the pocket suitable to receive hydrophobic groups. **B.** Gly. The dashed

black ring indicates the lack of hydrophobic-hydrophobic interactions. **C.** γ-Glu-Val-Gly. The

594 red dashed box indicates the additional polar contact between the peptide C-terminus (Gly

595 at the 3rd position) and the side chain of Asn102. **D.** γ-Glu-Val-Trp. The dashed black rings

596 indicate the lack of interaction with the residues engaged by the other molecules under

597 investigation. **E.** Docking pose superimposition of γ-Glu-Val-Gly (white), γ-Glu-Ile-Ala

598 (yellow), γ-Glu-Pro-Ser (green) and γ-Glu-Pro-Ala (cyan). **F.** Docking pose superimposition of

599 γ-Glu-Val-Trp (white), γ-Glu-Ile-Cys (yellow) and γ-Glu-Ile-Pro (green).
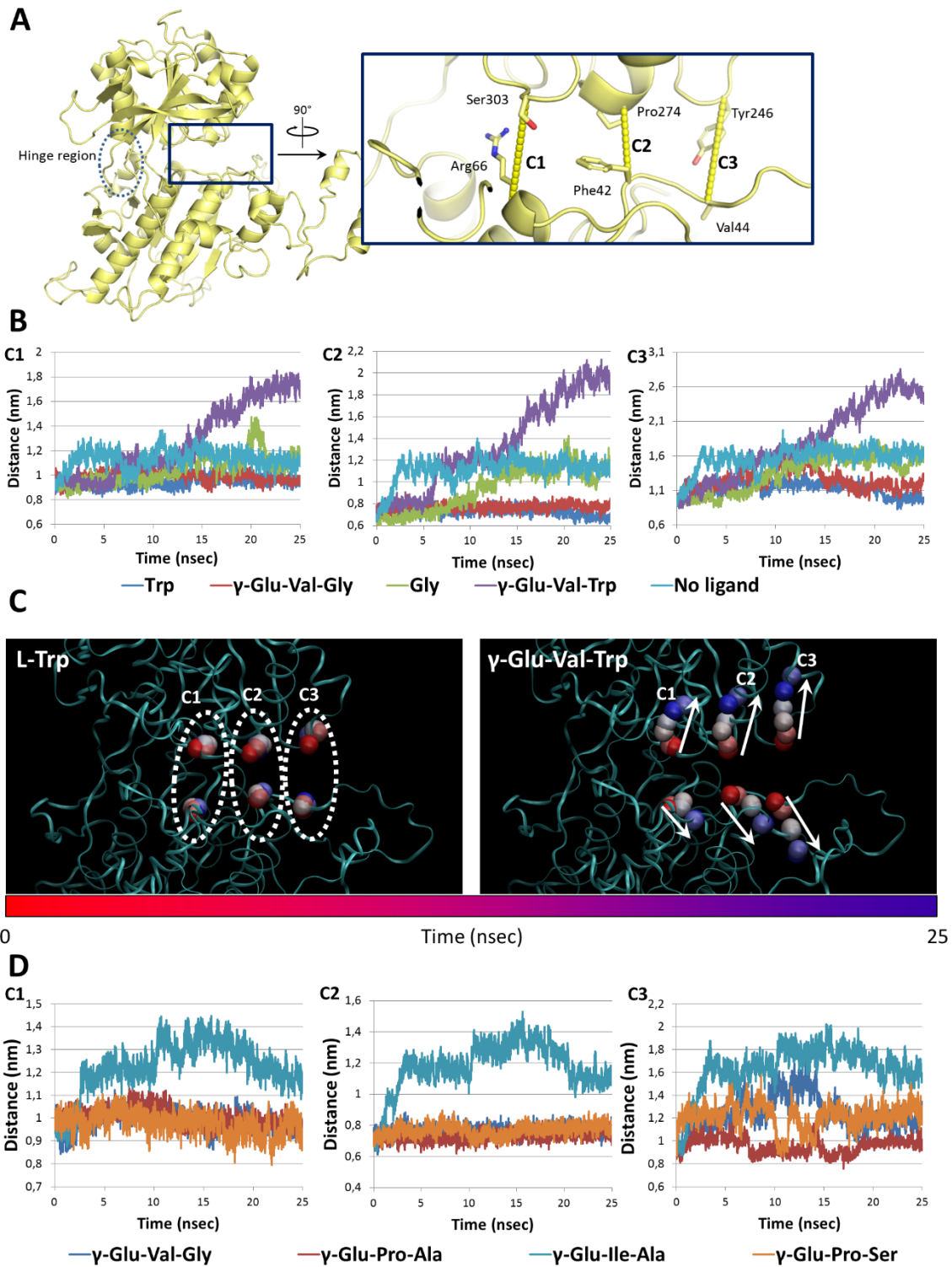
Figure 3. Molecular dynamics results. A. Graphical representation of CaSR in cartoon. The dashed ring indicates the hinge region while the three intra-molecular contact region distances considered to measure the opening of VFT domain are indicated with yellow dashed lines in the close-up on the right. Specifically, three contact regions (C1, C2 and C3) were defined between the α-carbon of Arg66-Ser303, Pro274-Phe42 and Tyr246-Val44,

30

606   respectively. **B.** Distance plots of C1, C2 and C3 contact regions for VTF domain in complex

607   with Gly, L-Trp, γ-Glu-Val-Gly, γ-Glu-Val-Trp or in the unbound state. **C.** Trajectory analysis of

608   contact region C1, C2 and C3 for VTF domain in complex with L-Trp or γ-Glu-Val-Trp. The

609   from-red-to-blue colour switch indicates the stepwise changes of coordinates during the

610   simulation. The dashed white rings indicate the stable fluctuation of interatomic distances

611   for C1, C2 and C3 contact regions when VTF domain was in complex with L-Trp. Conversely,

612   white arrows indicate the progressive detachment of C1, C2 and C3 contact regions for VTF

613   domain in complex with γ-Glu-Val-Trp leading to the structure opening. **D.** Distance plots of

614   C1, C2 and C3 contact regions for VTF domain in complex with γ-Glu-Val-Gly (taken as

615   reference), γ-Glu-Pro-Ala, γ-Glu-Ile-Ala or γ-Glu-Pro-Ser.

A
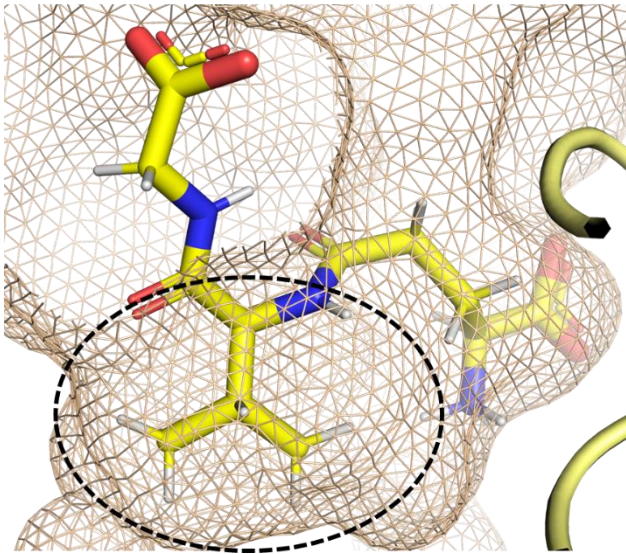
B
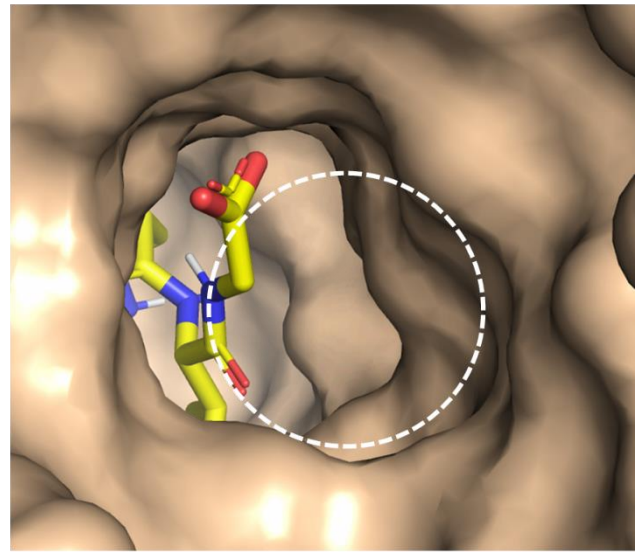
616
617 **Figure 4.** Close-ups of the pocket environment surrounding γ-Glu-Val-Gly. **A.** Focus on the

618 space surrounding the side chain of Val at the 2nd position. The pocket is represented in

619 mesh while γ-Glu-Val-Gly is represented in sticks. The black dashed ring indicates the almost

620 full sub-site occupancy by Val side chain. **B.** Focus on the space surrounding Gly at the 3rd

621 position. The pocket is represented in solid surface while γ-Glu-Val-Gly is represented in

622 sticks. The white dashed ring indicates the presence of a solvent exposed region of the VTF

623 domain binding site that could be occupied by the side chain of certain amino acids at the

624 3rd position of γ-Glutamyl tripeptides.

Tables

Table 1. Docking scores and reported activity of molecules under analysis

Peptide	Docking score (mean ± SD)[1]	Experimental activity
Gly	58.65 ± 0.04	Very weak activator[2]
L-Trp	103.37 ± 0.16	Moderate activator [3]
γ-Glu-Val-Gly	116.70 ± 0.90	Strong activator [4]
γ-Glu-Val-Trp	115.65 ± 4.14	Inactive [4]
γ-Glu-Pro-Ala	123.26 ± 0.86	Unknown
γ-Glu-Ile-Ala	121.86 ± 0.36	Unknown
γ-Glu-Pro-Ser	125.54 ± 1.16	Unknown
γ-Glu-Ile-Cys	124.41 ± 0.82	Unknown
γ-Glu-Ile-Pro	115.42 ± 0.39	Unknown

Note: [1] Docking scores are expressed as mean ± SD of three replicates. [2] According to (Geng et al., 2016). [3] According to (Conigrave et al., 2000). [4] According to (Ohsu et al., 2010).

626

Click here to access/download
Supplementary material for online publication only
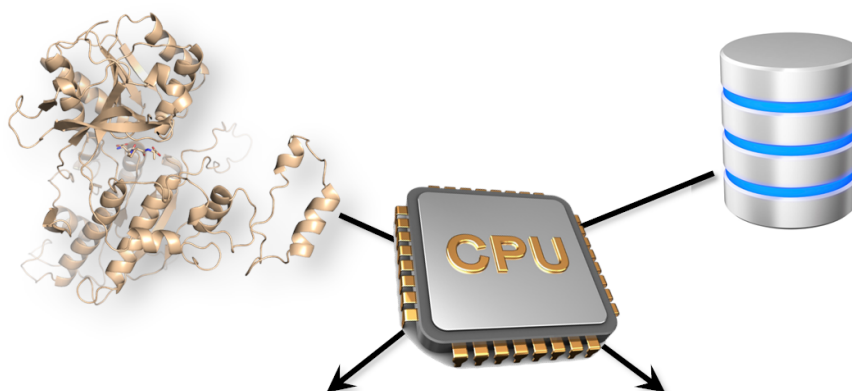R2_SM_Gustav_FRI.docx

Graphical abstract

A mechanistic investigation on kokumi-active γ-Glutamyl tripeptides

3D model of CaSR's venus flytrap domain

Virtual library of 400 γ-Glutamyl tripeptides

3D structure-activity relationship analysis of kokumi-active γ-Glutamyl tripeptides

Tool for the top-down identification of kokumi-active molecules

CRediT author statement

Luca Dellafiora: Conceptualization, Methodology, Software, Formal analysis, Investigation, Writing - Original Draft, Writing - Review & Editing, Supervision

Fabio Magnaghi: Methodology, Software, Formal analysis, Investigation, Writing - Original Draft

Gianni Galaverna: Conceptualization, Writing - Original Draft, Writing - Review & Editing

Chiara Dall'Asta: Conceptualization, Writing - Original Draft, Writing - Review & Editing, Supervision